

Stress-strain rate relation of agricultural soils

J. SHEN and R.L. KUSHWAHA

*Agricultural & Bioresource Engineering Department, University of Saskatchewan, Saskatoon, SK, Canada S7N 0W0.
Received 13 October 1993; accepted 30 August 1994.*

Shen, J. and Kushwaha, R.L. 1995. Stress-strain rate relation of agricultural soils. *Can. Agric. Eng.* 37:019-028. The stress-strain rate relation of agricultural soils was studied on the basis of statistical mechanics and experimental results from a modified triaxial apparatus. A model dealing with the dependence of stress on strain rate was developed. The model gave a satisfactory prediction on stress-strain rate behavior under shear loading conditions. The potential use of this model in constructing a stress-strain-time model is introduced.

Keywords: Rheology, soil mechanics, agricultural soils

La relation entre le stress et le taux de déformation de sols agricoles a été étudiée à l'aide de la mécanique statistique et de résultats expérimentaux obtenus avec un appareillage triaxial modifié. Un modèle de dépendance du stress sur le taux de déformation a été développé. Le modèle a prédit de façon satisfaisante le comportement du stress en fonction du taux de déformation pour des conditions de chargement créant du cisaillement. L'utilité potentielle de ce modèle pour le développement d'un modèle temporel de stress-déformation est introduit.

INTRODUCTION

Soil manipulation, including tillage, planting, and fertilization, is generally a dynamic process in which the rate effect on soil stress-strain relation should be considered in analytical modelling.

Since the 1950's, rheological properties of soils have been studied by many researchers (Geuze and Tan 1953; Gupta and Pandya 1966; Ram and Gupta 1972; Sudo et al. 1968; Pan 1986; Pan and Ji 1987; Pan et al. 1990). Most of these researchers adopted classical visco-elastic or viscoplastic models that included the following deficiencies:

- (a) Various types of visco-elastic models are mathematical combinations of basic elements (spring, dashpot, and slider). The choice of the number and combination form of basic elements is somewhat arbitrary. Reasonable agreement between the prediction by some models and actual soil behavior may not necessarily be considered as support for these models, since equations of these models depend only on the mathematical consequences of a particular arrangement of model elements that have been chosen (Singh and Mitchell 1968).
- (b) These models are phenomenological without a sound basis in physics.
- (c) These models are not well suited to describing the stress-strain behaviour of unsaturated soils, since stress is generally considered linear with strain in these models and extensive indoor and outdoor tests have indicated that this kind of linearity does not exist with unsaturated soils (Bekker 1969).

Agricultural soils are a non-uniform medium in which the size and configuration of solid particles, the granular struc-

ture formed by a considerable number of particles, and the interactions among air, water, and particles vary tremendously from place to place within the soil. After soil is subjected to an external load, the breakage of particles, the air and water being squeezed from soil, and the destruction of the original granular structure due to particles sliding and rolling over each other results in additional complexities. Currently, the development of a model that can account for the forgoing features of soil appears very difficult. One reasonable approach to the mechanical behavior of soil is to neglect the subtle changes in the soil at specific points and to discuss the average behaviour of soil on a probability basis.

Statistical mechanics is based on probability and universally suited for describing various types of mechanical systems. Therefore, in this study it was used as a fundamental basis for investigating the stress-strain rate relation for agricultural soils and was evaluated by laboratory experiment.

TERMS AND ASSUMPTIONS

Element of soil structure

According to the theory of the double electric layer formulated by Gouy (1910) and further developed by Chapman (1913), a solid particle, especially a colloidal particle, is in conjunction with a layer, a few molecules thick, of firmly-bound (adsorbed) water comprising positive ions (cations), as shown in Fig. 1 (Vyalov 1986). Beyond this layer, there exists a layer of loosely-bound (lysisorbed) water which also consists of positive ions of water and flows along the surface of a soil particle in the course of deformation. The firmly-bound and loosely-bound water form a double layer, several nanometres thick. Outside this double layer, free water or air is located. In this study, a soil particle and its surrounding double layer of water are defined as an element of soil structure.

Force and potential energy in particle interaction

Each particle is subjected to external and internal forces as well as to fields of energy induced by these forces. Internal fields are produced by interparticle forces between soil elements. In general, inter and intra-particle forces in soil include: chemical forces, molecular forces, ionic-electrostatic forces, capillary-electrostatic (Coulomb) forces, and magnetic forces (Vyalov 1986). These forces produce fields of energy and form bonds between particles of a dispersed system. For soil with a stable structure, forces of particle interaction are of two types: forces of attraction, f_a , which make particles gather together and forces of repulsion, f_r , which prevent annexation of particles. The forces of attrac-

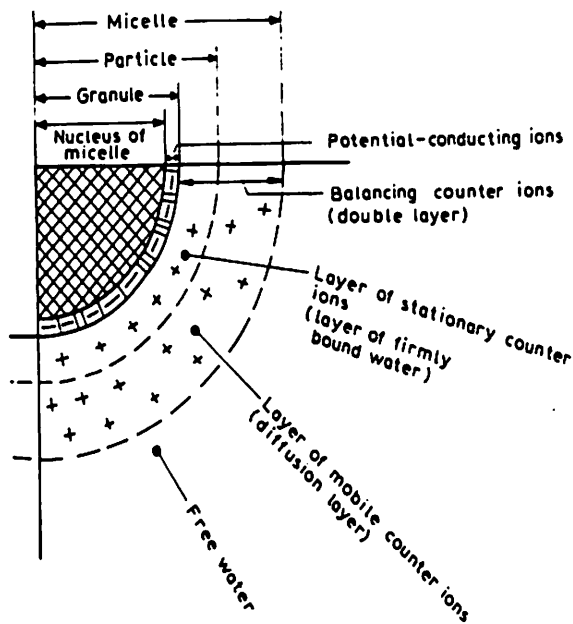
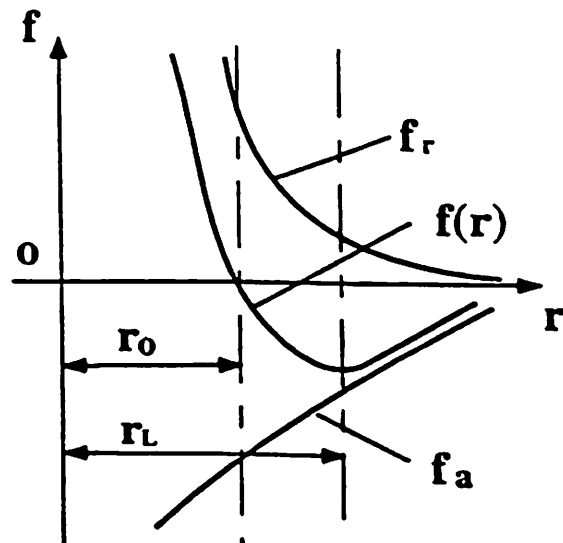


Fig. 1. Electromolecular forces of a mineral particle and the hydrated envelope (Vyalov 1986).

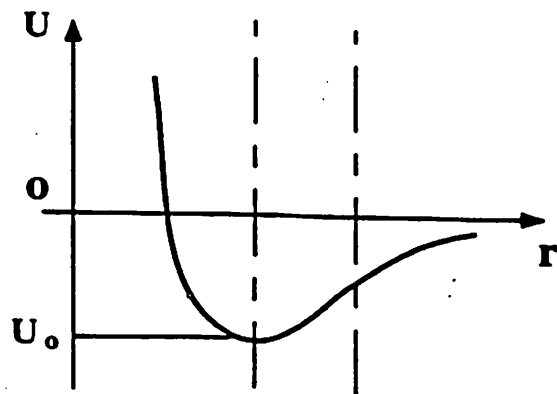
tion and repulsion differ among soil types. To bond particles into a soil structure, the resultant force, f , and potential energy, U , of particle interaction in different soil types have some common features, as shown in Fig. 2a. When r is large, the absolute value of f_a increases more rapidly than f_r decreases with r . Consequently, the resultant force $f(r)$ is less than zero and attractive, which makes particles gather together. When r is relatively small, f_r increases more rapidly than f_a decreases with r . As a result, $f(r)$ is larger than zero and repulsive, which avoids the annexation of particles. When $r = r_0$, f_a is equal to f_r and f equals zero (Fig. 2a). Since $dU(r)/dr = -f(r)$, curve $U(r)$ can be obtained from $f(r)$ (Fig. 2b). When $r = r_0$, $dU(r)/dr$ equals zero, and the potential energy reaches its minimum value, U_0 . Thus, two particles separated by a distance r_0 are in equilibrium.

Idealization of soil shear process

As mentioned before, there is usually a layer of firmly-bound water, a few molecules thick, surrounding soil particles. It is almost impossible for an external force to pull this water off the surface of particles, because forces of attraction between a soil particle and its firmly-bound water may reach 1 GPa (Vyalov 1986). The layer of loosely-bound water is removable from the surface of a particle. During a shear process, a certain amount of normal stress is applied on the double layer of a particle and may force the loosely-bound water off the surface of a particle. For simplicity, the boundary interface of a particle in shear process is idealized as a single layer of positive ions of water attached to the particle. The distance between two boundary interfaces belonging to two adjacent particles is defined as the distance between these two particles, as shown in Fig. 3. This distance decreases with the increase in compressive stresses applied on the double layer of two adjacent particles and can not become zero because of the repulsion between positive ions in the two boundary



(a)



(b)

Fig. 2. Balance between interparticle forces.

interfaces. In the equilibrium of external compressive forces, the distance between two adjacent particles equals a quantity of the same magnitude as r_0 in Fig. 2.

The relative displacement between two particles in a shear process can then be simplified as the relative movement of two layers of cations belonging to two adjacent particles at a uniform shear plane. The direction and area of this plane depend on contact types between the particles (edge-to-edge, edge-to-face, or face-to-face) and the relative position of the particles in rolling over each other in a shear process. Since the contact type and relative position between particles are generally random in soil, actual shear planes between particles in soil may exist in every direction with different contact areas. However, in a statistical sense, an average shear plane between two groups of particles should be definite in both direction and area. For example, the tangential direction of the average shear plane for a specimen in a direct shear test is normal to the axis of the cylindrical specimen and the area

APPLICATION OF STATISTICAL MECHANICS IN ANALYZING SHEAR PROCESS

Statistical mechanics has been used to study the rate-dependent deformation of such materials as ceramics (Gibbs and Eyring 1949), metals (Finnie and Heller 1959), plastics and rubber (Ree and Eyring 1958), textiles (Eyring and Halsey 1948), asphalt (Herrin and Jones 1963), and concrete (Polivka and Best 1960). It has also been adopted for the study of viscosity, plasticity, friction, lubrication, and diffusion (Eyring and Powell 1944).

Soil consists of a great number of particles per unit volume. Different shapes and sizes of particles and different contact types and relative positions between particles lead to non-uniformly distributed heat energy between different particles in soil. Under such circumstances, the pattern of average distribution of the energy between particles may be described in terms of the Boltzmann distribution law in statistical mechanics (Vyalov 1986).

The approach to stress-strain rate relation in this research was a combination of theoretical analysis and experiment. The stress-strain rate equation was initially obtained and simplified from a theoretical analysis and then verified on the basis of experimental data.

Average crossing frequency of particles

A thermo-vibration process takes place both in the lattice of mineral particles and in the molecular structure of firmly-bound water film interlinking particles (Vyalov 1986). More often, external forces are only a very small fraction of intracrystalline forces of mineral particles and are thus incapable of causing an oriented displacement inside particles. However, these external forces are quite adequate to activate cations in the bound water layer to form an oriented displacement. Therefore, most soil deformation is due to the relative movement between particles.

Average translation speed of atoms N_0 random thermal vibrations of cations in a contact zone between two soil particles are taken as an observation sample. This sample is actually a system composed of quasi-independent subsystems. One-dimensional vibration of cations of water along the contact zone between particles contributes the most to the micro-displacement of particles. Therefore, random thermal vibration of cations is idealized to one-dimensional movement of a free particle in a box with the length equal to the interval distance of atoms. According to the Schrödinger wave equation (Glasstone et al. 1941), the average moving speed \dot{x}_a of cations along the positive x direction can be obtained after several derivations as:

$$\dot{x}_a = \left(\frac{kT}{2\pi M} \right)^{0.5} \quad (1)$$

where:

- k = Boltzmann's constant,
- T = absolute temperature, and
- M = atom mass.

If a is the interval distance of cations of firmly-bound water, the number of energy barriers crossed over per unit time, N_u , is:

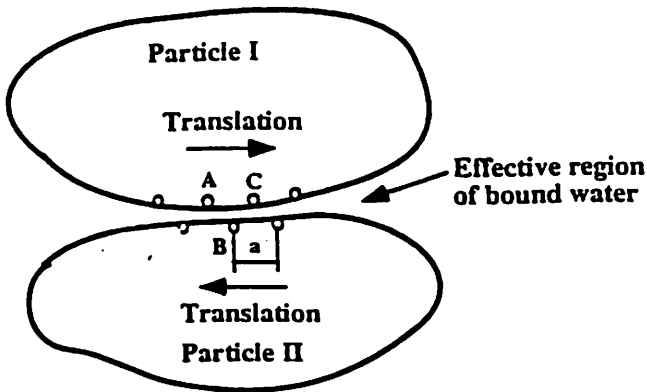


Fig. 3. Model for interaction between particles.

of this average shear plane equals the cross sectional area of the soil specimen. If probabilities of the relative movement between two particles in both forward and backward directions along the average shear plane are known, the average shear strain rate of soil can be calculated on a probability basis. In this study, a uniform shear plane was adopted to simplify the boundary surface formed by two particles, as shown in Fig. 3. Cations A and B in Fig. 3 represent positive ions of firmly-bound water of particle I and particle II, respectively.

If external forces are large enough, cation A and particle I will move, relative to particle II, a distance a which equals the interval distance of two adjacent cations in a layer of bound water. In this relative movement, when the line connecting cations A and B is perpendicular to the moving direction, the distance between A and B reaches its minimum value and the force of repulsion becomes maximum. The difference between the potential energy corresponding to maximum repulsion and that in the original equilibrium is called the barrier of potential energy. Cations are constrained from movement relative to each other by virtue of energy barriers separating adjacent equilibrium positions by a distance between atoms, as depicted schematically in Fig. 4. The displacement of cations to new positions requires sufficient magnitude of activation energy ΔF_a to overcome the barriers. After moving to equilibrium position 2 from position 1, if external potential is large enough, a cation will continuously move to the position 3, 4 and so on. This forms irreversible macro-deformation in soil.

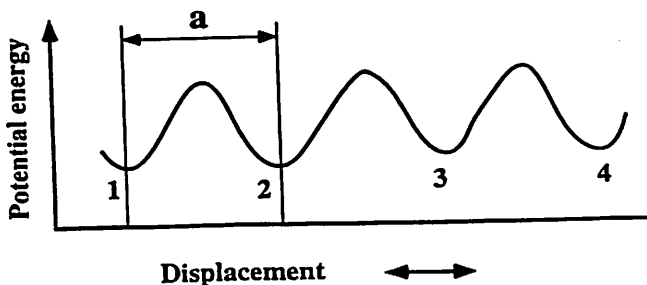


Fig. 4. Potential barriers and displacement.

$$N_u = \frac{\dot{x}_a}{a} = \frac{1}{a} \left(\frac{kT}{2\pi M} \right)^{0.5} \quad (2)$$

In this study, a has been assumed to be a value of 0.28 nm, that is the same as the distance separating atomic valleys in the surface of a silicate mineral.

Translation partition function The one-dimensional translation partition function, f_x , can be written as (Eyring and Powell 1944):

$$f_x = \sum \omega_x \exp \left(-\frac{E_x}{kT} \right) \quad (3)$$

where:

E_x = one-dimensional particle energy, and
 ω_x = number of quantum state.

Vibrating frequency of atoms The product of f_x and N_u leads to the vibrating frequency of atoms, V_o , in the following form:

$$V_o = N_u f_x = \frac{kT}{h} \quad (4)$$

where h = Plank's constant.

Average probability and frequency for soil particle's overcoming energy barrier

When the soil body is in an equilibrium state, cations of bound water at the interface between adjacent particles may cross one or several energy barriers by accidental thermal fluctuation. However, since the probability for these cations to cross energy barriers in both forward and backward directions is the same, no macro-deformation results. In the process of crossing one energy barrier by a particle, the introduction of an activation energy, ΔF , of sufficient magnitude is required. Here, ΔF is a function of contact zone and relative position between particles as well as external loads applied on the contact zone. The potential energy of a particle may be the same following the activation process, or higher or lower than its initial value.

On the basis of the theory of absolute reaction rates by Eyring (1936) and Glasstone et al. (1941), the average probability, ρ , for soil particle's overcoming energy barrier can be derived, on the basis of the Boltzmann distribution law, as:

$$\rho = \exp \left(-\frac{\Delta F}{NkT} \right) \quad (5)$$

where N is Avogadro's number (6.02×10^{23}). If an entire soil body is analyzed, ΔF in Eq. 5 should be the average value for all particles. The adaptation of the theory of absolute reaction rates to the study of soil behavior in civil engineering was given by Abdel-Hady and Herrin (1966), Andersland and Douglas (1970), Christensen and Wu (1964), Mitchell (1964), Mitchell et al. (1968, 1969), Murayama and Shibata (1958, 1961, 1964), Noble and Demirel (1969) and Wu et al. (1966).

The product of the vibrating frequency kT/h (Eq. 4) and the probability ρ (Eq. 5) determines the number of barriers surmounted by a particle per unit time, namely crossing

frequency ν , as (Mitchell 1976):

$$\nu = \frac{kT}{h} \exp \left(-\frac{\Delta F}{NkT} \right) \quad (6)$$

In the absence of directional potentials, barriers are crossed with an equal frequency in all directions and no macro-displacement can be observed. If, however, a directed potential is applied, then the frequency in the direction of the potential and the opposite direction changes.

Shear

To simulate a pure shear case, consider a soil body with a unit volume in Fig. 5 in which surfaces A and C are subject to a pressure P ($P > 0$), and surfaces B and D are subject to a tensile stress $-P$. The force component p_p induced by the average allocation of the pressure P to each particle in the direction of P may be written as:

$$P_p = \frac{P}{N_a} \quad (7)$$

where N_a = number of particles per unit area and assumed constant unless particles break down or volumetric compression occurs.

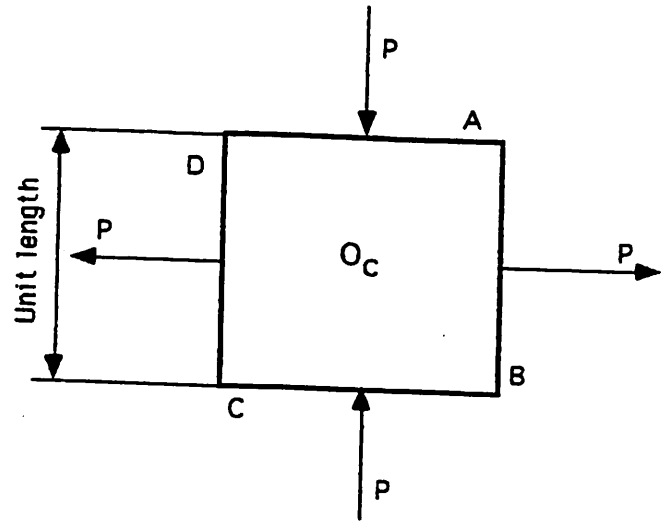


Fig. 5. Analytical unit for shear.

In a process in which a particle on a surface of a soil body crosses a barrier toward the centre of a soil body, the pressure P exerted on the surface will exert a work equal to $p_p \times a$ (a : distance between cations of bound water), and the frequency of a particle's crossing a barrier from the surface A or C to the centre can be expressed as (Mitchell 1976):

$$\nu_i (A \rightarrow O_c) = \nu_i (C \rightarrow O_c) = V_o \exp \left(\frac{-\Delta F/N + p_p a}{kT} \right) \quad (8)$$

For a tensile stress, the frequency of a particle's crossing a barrier from the surface B or D to the centre can be expressed as:

$$\nu_i (B \rightarrow O_c) = \nu_i (D \rightarrow O_c) = V_o \exp \left(\frac{-\Delta F/N - p_p a}{kT} \right) \quad (9)$$

In Eqs. 8 and 9, $v_i(A \rightarrow O_c)$ and $v_i(C \rightarrow O_c)$ are average crossing frequencies of particles on surfaces A and C to the centre respectively; and $v_i(B \rightarrow O_c)$ and $v_i(D \rightarrow O_c)$ are average crossing frequencies of particles on surfaces B and D to the centre, respectively.

The average translational velocity of particles on each surface is given by:

$$V_i(A \rightarrow O_c) = V_i(C \rightarrow O_c) = a V_0 \exp\left(\frac{-\Delta F/N + p_p a}{kT}\right)$$

$$V_i(B \rightarrow O_c) = V_i(D \rightarrow O_c) = a V_0 \exp\left(\frac{-\Delta F/N - p_p a}{kT}\right) \quad (10)$$

where $V_i(A \rightarrow O_c)$ and $V_i(C \rightarrow O_c)$ = average translational velocities to the centre of particles on surfaces A and C; $V_i(B \rightarrow O_c)$ and $V_i(D \rightarrow O_c)$ are the velocities to the centre of particles on surfaces B and D, respectively.

The gradients of average velocity along four shear directions are:

$$\nabla V_i(A \rightarrow B) = \nabla V_i(C \rightarrow B) = \nabla V_i(A \rightarrow D) = \nabla V_i(C \rightarrow D)$$

$$= -2aV_0 \exp\left(-\frac{\Delta F}{NkT}\right) \sinh\left(\frac{p_p a}{kT}\right) \quad (11)$$

$-\nabla V_i$ is actually proportional to the shear strain rate of relative sliding caused by particles crossing barriers and is given by:

$$\dot{\gamma} = -\lambda_0 \nabla V_i(A \rightarrow B) = \lambda \exp\left(-\frac{\Delta F}{NkT}\right) \sinh\left(\frac{P a}{kTN_a}\right) \quad (12)$$

where,

$$\lambda = -\frac{2\lambda_0 a k T}{h} \quad (13)$$

and $\dot{\gamma}$ is shear strain rate and λ_0 is assumed to be a constant for a specific deformation process. Equation 12 is the stress-strain rate relation derived on the basis of statistical mechanics for a shear case.

EQUATION SIMPLICITY AND EXPERIMENTAL EVALUATION

In Eq. 12, the expression $\sinh(Pxa/(kxTxNa))$ makes the application of this equation complicated. According to typical values of parameters in Eq. 12, the equation form is simplified in the following. The simplified stress-strain rate equation is then evaluated with experimental data.

Equation simplicity

Typical values of $Pxa/(kxTxNa)$ for clay, silt, and sand are listed in Table I. In Table I, the number of particles per unit area for clay is assumed to be $5.9 \times 10^{13} \text{ m}^{-2}$ (Mitchell 1964) and proportional to $1/d^2$ where d equals the diameter of the particles. The pressure P is assumed to be a value of 10 kPa which is usually encountered in agricultural production. Table I indicates that the values of $Pxa/(kxTxNa)$ for various types of soil are usually greater than one. Therefore, $\sinh(Pxa/(kxTxNa))$ can be approximately replaced by

$\exp(Pxa/(kxTxNa))$. Equation 12 could then be written as:

$$\dot{\gamma} = \frac{\lambda}{2} \exp\left(-\frac{\Delta F}{NkT}\right) \exp\left(\frac{P a}{kTN_a}\right) \quad \text{shear } (P = \tau) \quad (14)$$

Taking the natural logarithm of both sides in Eq. 14 and substituting τ for P leads to:

$$\ln \dot{\gamma} = \ln\left(\frac{\lambda}{2}\right) - \frac{\Delta F}{NkT} + \frac{a \tau}{kTN_a}$$

$$= A + \alpha \tau \quad (15)$$

where:

$$A = \ln\left(-\frac{\lambda_0 a k T}{h}\right) - \frac{\Delta F}{NkT}$$

$$\alpha = \frac{a}{kTN_a} \quad (16)$$

Table I. Values of some parameters in Eq. 12

	Clay	Silt	Sand
k (Nm K ⁻¹)	1.38 x 10 ⁻²³	1.38 x 10 ⁻²³	1.38 x 10 ⁻²³
T (K)	300	300	300
P (Nm ⁻²)	10 ⁴	10 ⁴	10 ⁴
a (m)	2.8 x 10 ⁻¹⁰	2.8 x 10 ⁻¹⁰	2.8 x 10 ⁻¹⁰
d (m)	10 ⁻⁶	2 x 10 ⁻⁵	4 x 10 ⁻⁴
Na (m ⁻²)	5.9 x 10 ¹³	1.47 x 10 ¹¹	3.83 x 10 ⁸
Pa/(kTNa)	11.46	4.58 x 10 ³	1.76 x 10 ⁶

Experimental evaluation

Three types of test soil (light loam, silty clay, and clay) were used. Constant stress and constant strain-rate tests were conducted by a modified triaxial apparatus. Since the confining pressure of specimens was maintained constant during triaxial tests, axial stress and strain of the soil specimens can be considered proportional to the shear stress and strain of specimens, respectively. Therefore, if the linearity between axial stress and logarithm of axial strain of soil specimens can be proved, then the relation between shear stress and logarithm of shear strain is considered to be linear.

Constant stress test with a constant environmental temperature

In a constant stress test, external loads and environmental temperature are constant. Since the strain rate in the tests was not very high, the temperature change in the soil specimens during a deformation process can be neglected.

In the case of constant external stresses and environmental temperature, there is only one variant ΔF on the right-hand side of the expression of parameter A in Eq. 16 and ΔF is mainly related to the orientation of soil particles.

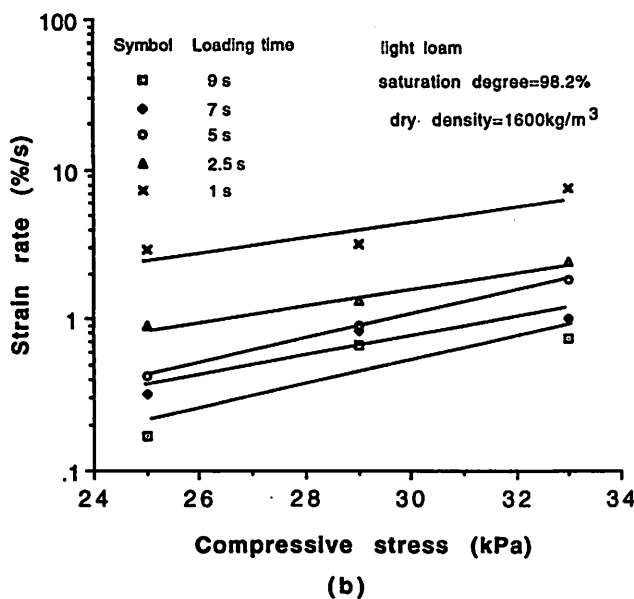
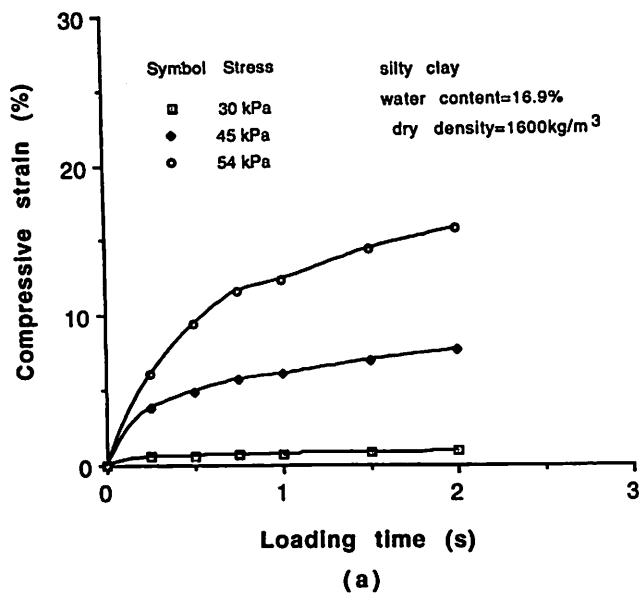


Fig. 6. Results of unconfined compression test at constant stress.

Similarly, there is only one variant N_a on the right-hand side of the expression of parameter α in Eq. 16, and N_a is also mainly dependent on the orientation of soil particles if particles are seldom broken down.

Maximyak (1968) conducted a series of creep tests on identical specimens of clay and focused his attention on the changes in micro-structure at various stages of deformation. According to his experimental data, the orientation of soil particles at different loads but for the same period of loading time appeared to be roughly the same. Therefore, it may be assumed that in a first approximation the orientation of soil particles is not influenced directly by the applied stresses and is governed, mainly, by the loading time. On the basis of this assumption and the discussion in the last paragraph, it is

reasonable to expect that parameters A and α in Eq. 16 are mainly controlled by loading time, t , and for any arbitrary t , $\ln \dot{\gamma}$ should have a linear relation with τ .

For unconfined tests, Fig. 6(a) shows experimental curves of silty clay and Fig. 6(b) illustrates experimental results of light loam. At different loading times, the logarithm of axial strain rate has a linear relation with axial stress. Figure 7 shows the results of confined tests with silty clay. The linear regression results of Eq. 15 for each line in Figs. 5 and 6 are listed in Table II which indicates that the logarithm of axial strain rate has an approximately linear relation with shear stress.

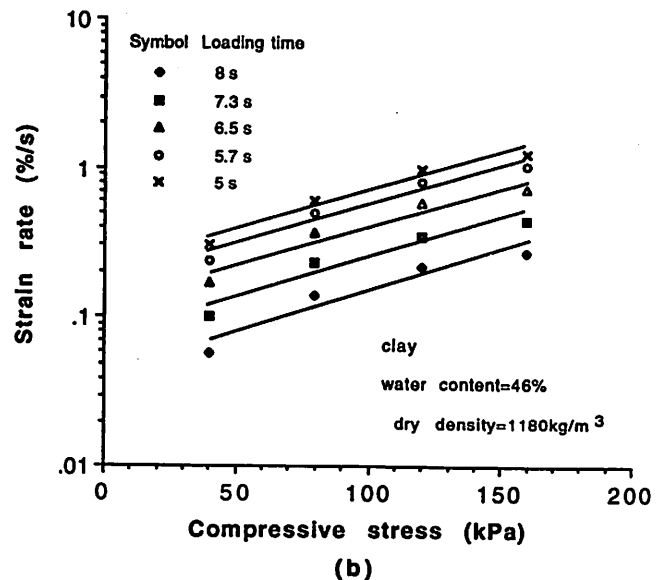
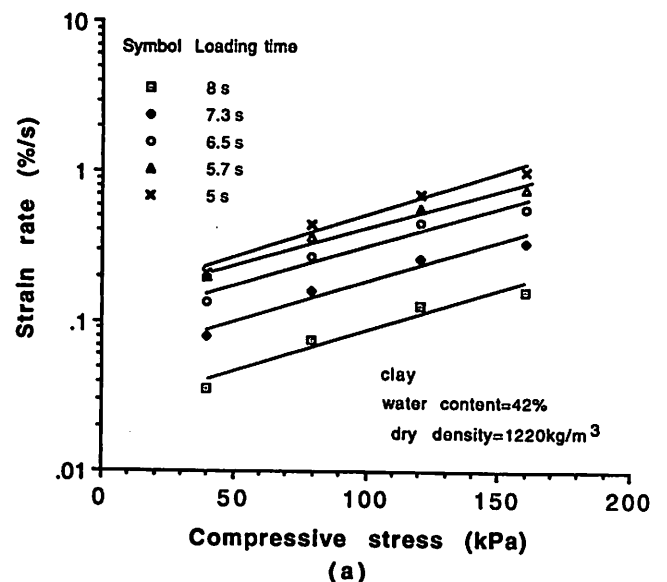


Fig. 7. Results of confined compression test at constant stress.

Table II. Regression results of Eq. (15) for constant stress tests

Figure No.	Loading time (s)	A (ln(%s ⁻¹))	α (ln(% s ⁻¹)/kPa)	R ²
6 (b)	1	- 6.204	0.185	0.802
6 (b)	2.5	- 4.630	0.145	0.877
6 (b)	5	- 5.470	0.185	0.999
6 (b)	7	- 3.222	0.123	0.981
6 (b)	9	- 1.964	0.117	0.804
7 (a)	5	- 3.684	0.0123	0.945
7 (a)	5.7	- 2.919	0.0121	0.955
7 (a)	6.5	- 2.378	0.0121	0.950
7 (a)	7.3	- 1.991	0.0113	0.973
7 (a)	8	- 1.974	0.0129	0.972
7 (b)	5	- 3.169	0.0126	0.916
7 (b)	5.7	- 2.616	0.0121	0.921
7 (b)	6.5	- 2.094	0.0119	0.928
7 (b)	7.3	- 1.789	0.0122	0.947
7 (b)	8	- 1.561	0.0119	0.959

Constant strain-rate test with a constant environmental temperature

In a constant strain-rate test with a constant environmental temperature, strain rate of soil specimens is assumed to be constant. All parameters on the right-hand sides in Eq. 16 are constants except for Δ*F* and *N_a*. The change of Δ*F* and *N_a* mainly depends on the change in soil structure. For a constant strain-rate test, strain is proportional to loading time and thus appears to be the most useful single parameter for characterizing the change in soil structure, Δ*F* and *N_a*. Therefore, at an arbitrary strain, ln $\dot{\gamma}$ should have a linear relation with τ.

The experimental stress-strain rate relations of unconfined triaxial tests with light loam and silt clay are illustrated in Fig. 8. In Fig 8, strain of soil specimens ranges from 1% to 8%.

The results of confined triaxial tests with saturated light loam are shown in Fig. 9 in which each straight line represents a stress-strain rate relation obtained at a certain strain.

The shear strength-strain rate relation is a special case of shear stress-strain rate relation. The results of triaxial tests under confined conditions are shown in Fig. 10, which indicates that shear strength has a linear relation with logarithm of axial strain rate for clay.

The values of parameters *A*, α, and R² for each line in Figs. 8 and 9 are listed in Table III and those for each line in Fig. 10 are listed in Table IV. An approximately linear relation exists in all cases.

APPLICATION OF THE EQUATION IN CONSTRUCTING A STRESS-STRAIN-TIME EQUATION

Since strain rate $\dot{\epsilon}$ is a function of stress, *P*, and loading time, *t*, Eq. 15 may be rewritten as:

$$\ln \dot{\epsilon}(t, P) = \ln \dot{\epsilon}(t, P_0) + \alpha P \tag{17}$$

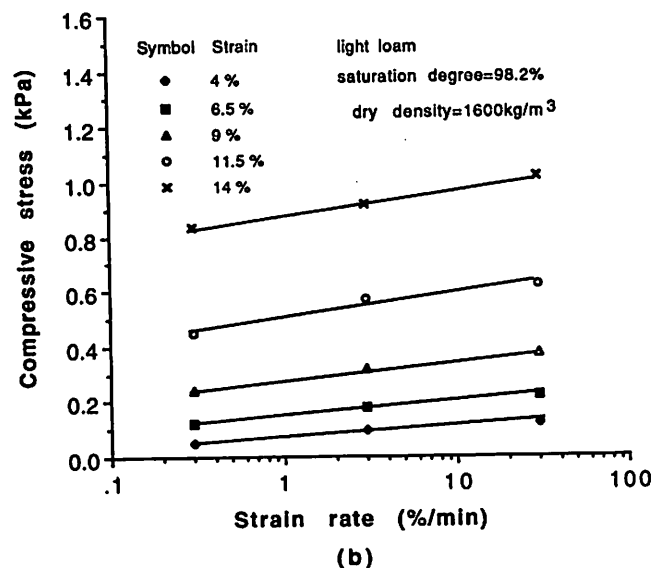
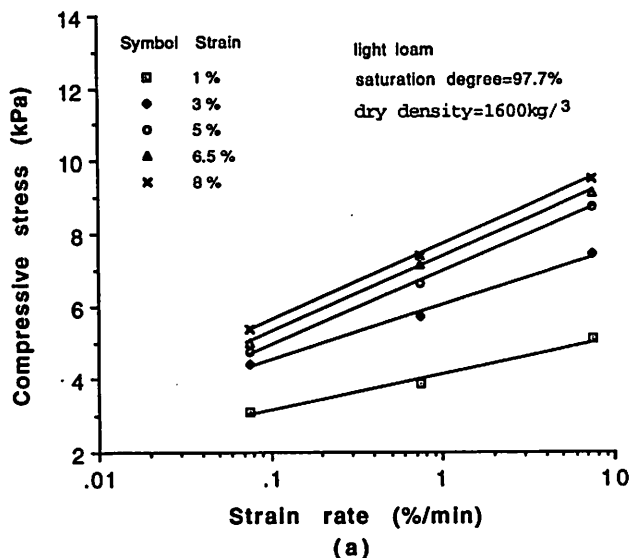


Fig. 8. Results of unconfined compression test at constant strain rate.

where:

$\dot{\epsilon}(t, P_0)$ = fictitious value of strain rate at *P*=0, a function of loading time, *t*, and

α = value of slope of the linear portion on the logarithmic strain rate versus stress plot.

According to Shen and Yu (1989), the strain rate-time equation for agricultural soil can be expressed by:

$$\ln \dot{\epsilon} = B - m \ln t \tag{18}$$

where *B*, *m* = coefficients.

Also, because $\dot{\epsilon}$ is a function of stress *P* and loading time *t*, Eq. 18 can be rewritten as:

Table III. Regression results of Eq. 15 for constant strain-rate tests

Figure No.	Strain (%)	A (ln (% s ⁻¹))	α (ln(% s ⁻¹)/kPa)	R ²
8 (a)	1	-9.615	2.314	0.985
8 (a)	3	-9.078	1.507	0.991
8 (a)	5	-8.032	1.155	0.999
8 (a)	6.5	-8.154	1.144	0.999
8 (a)	8	-8.499	1.107	0.999
8 (b)	1	-7.637	2.792	0.995
8 (b)	3	-9.855	2.488	0.997
8 (b)	5	-10.148	2.189	0.999
8 (b)	6	-9.492	1.893	0.990
8 (b)	7	-8.432	1.562	0.999
8 (b)	8	-7.937	1.379	0.998
9 (a)	4	-2.405	0.0955	0.975
9 (a)	6	-4.751	0.0868	0.999
9 (a)	8	-6.285	0.0690	0.989
9 (a)	10	-9.676	0.0575	0.999
9 (a)	12	-11.254	0.0395	0.995
9 (b)	14	-13.014	0.0255	0.991
9 (b)	4	-4.272	0.0610	0.981
9 (b)	6.5	-6.762	0.0450	0.997
9 (b)	9	-9.808	0.0351	0.992
9 (b)	11.5	-12.976	0.0257	0.961
9 (b)	14	-21.854	0.0248	0.996

Table IV. Regression results of Eq. 15 for shear strength versus strain rate relation

Figure No.	Confining pressure (kPa)	A (ln (% s ⁻¹))	α (ln(% s ⁻¹)/kPa)	R ²
10 (a)	30	-7.051	0.174	0.975
10 (a)	40	-9.647	0.162	0.878
10 (a)	50	-13.966	0.177	0.867
10 (a)	60	-23.430	0.242	0.925
10 (a)	70	-28.736	0.250	0.952
10 (a)	80	-26.868	0.199	0.969

$$\ln \dot{\epsilon}(t, P) = \ln \dot{\epsilon}(t_1, P) - m \ln \left(\frac{t}{t_1} \right) \quad (19)$$

where $\dot{\epsilon}(t_1, P)$ = value of strain rate at unit time, a function of stress P . By combining Eqs. 18 and 19 and noticing certain specific features of agricultural soil, a general stress-strain-time equation for agricultural soil can be expressed by (Shen and Yu 1990):

$$\epsilon = A_1 + A_2 \exp(A_3 P) T^{A_4} \quad (20)$$

where A_1, A_2, A_3, A_4 = parameters of Eq. 20.

The results of soil bin tests showed that Eq. 20 has the following advantages over the rheological equation of Bur-

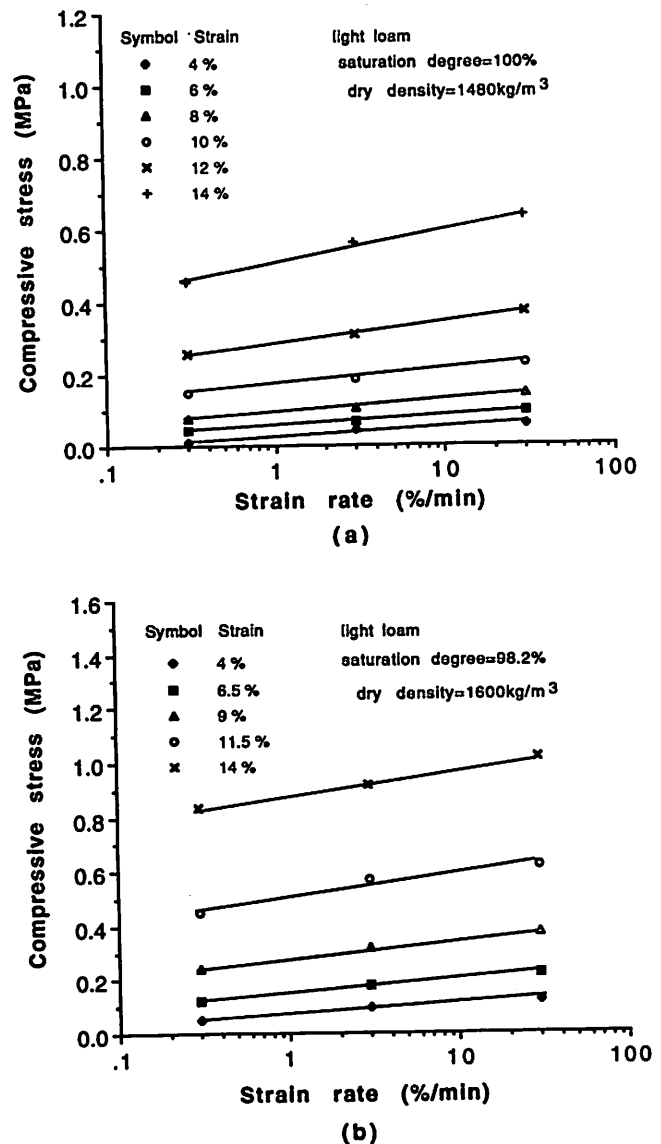


Fig. 9. Results of confined compression test at constant strain rate.

gers model (Shen and Yu 1990):

- (1) based on experimental results at two different pressures, sinkage behavior at other pressures can be predicted more accurately;
- (2) the form of Eq. 20 is simple and its parameters are easy to determine from test results;
- (3) equation 20 is well suited in describing the stress-strain behavior of both saturated and unsaturated soils.

CONCLUSIONS

A shear stress-strain rate equation was derived on the basis of statistical mechanics and simplified according to some features of soil and loading range in agricultural production.

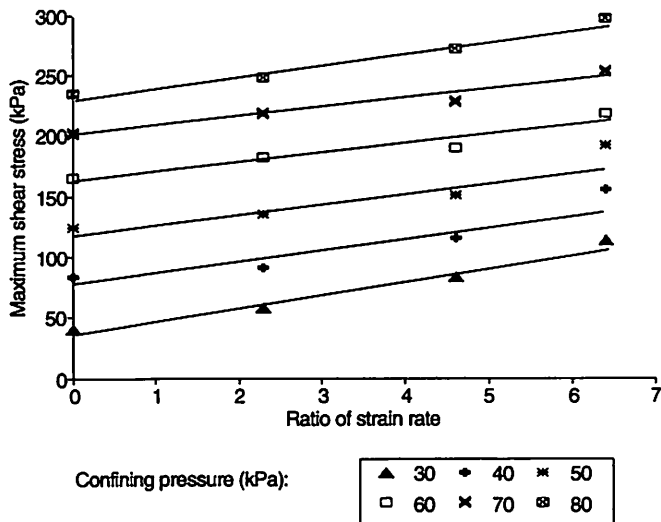


Fig. 10. Relation between shear strength and shear strain rate with clay.

Constant stress and constant strain-rate tests were conducted on a modified triaxial apparatus and the validity of the simplified equation was verified by experimental data. The basic form of the simplified equation is the same for different tests and is given by:

$$\ln \dot{\gamma} = A + \alpha \tau$$

where A , α = parameters depend on soil temperature, soil structure, loading time, or loading rate, etc. $\dot{\gamma}$ and τ are shear strain rate and stress (or strength), respectively. This relation will be useful in constructing a stress-strain-time model for agricultural soil.

ACKNOWLEDGMENTS

The authors gratefully acknowledge the financial assistance received from the Natural Sciences and Engineering Research Council of Canada and the President's NSERC Fund which partially funded this research.

REFERENCES

- Abdel-Hady, M. and M. Herrin. 1966. Characteristics of soil asphalt as a rate process. *Journal of the Highway Division, ASCE* 92(HW1):49-69.
- Andersland, O.B. and A.G. Douglas. 1970. Soil deformation rates and activation energies. *Geotechnique* 20(1):1-16.
- Bekker, M.G. 1969. *Introduction to Terrain-Vehicle Systems*. Ann Arbor, MI: The University of Michigan Press.
- Chapman, D.L. 1913. A contribution to the theory of electrocapillarity. *Philosophical Magazine* 25(6):475-481.
- Christensen, R.W. and T.H. Wu. 1964. Analyses of clay deformation as a rate process. *Journal of the Soil Mechanics and Foundations Division, ASCE* 90(6):125-157.
- Eyring, H. 1936. Viscosity, plasticity, and diffusion as examples of absolute reaction rates. *Journal of Chemical Physics* 4(4):283-291.

- Eyring, H. and G. Halsey. 1948. The mechanical properties of textiles - The simple non-newtonian model. In *High Polymer Physics*, 61-116. Chemical Rubber Co., Cleveland, OH.
- Eyring, H. and R. Powell. 1944. Rheological properties of simple and colloidal systems. *Alexander's Colloid Chemistry* 5:236-252.
- Finnie, I. and W. Heller. 1959. *Creep of Engineering Materials*. New York, NY: McGraw-Hill Book Co.
- Geuze, E.C.W.A. and T-K. Tan. 1953. The mechanical behaviour of clays. In *Proceedings of the 2nd International Conference on Rheology*, 247. Oxford, England.
- Gibbs, P. and H. Eyring. 1949. A theory for creep of ceramic bodies under constant load. *Canadian Journal of Science* 27:374-386.
- Glasstone, S., K. Laidler and H. Eyring. 1941. *The Theory of Rate Processes*. New York, NY: McGraw-Hill Book Co.
- Gouy, G. 1910. Sur la constitution de la electrique à la surface d'un electrolyte. *Annuie Physique (Paris), Serie 4* 9:457-468.
- Gupta, C.P. and A.C. Pandya. 1966. Rheological behaviour of soil under static loading. *Transactions of the ASAE* 9:718-724.
- Herrin, M. and G. Jones. 1963. The behavior of bituminous materials from the viewpoint of the absolute rate theory. In *Proceedings of the Association of Asphalt Paving Technologists*, 82-105. The Association of Asphalt Paving Technologists, Ann Arbor, MI.
- Maximyak, R.V. 1968. Structural changes in clay soil due to deformation. In *Collective Volume: Foundations and Underground Structures* (in Russian). Foundations and Underground Structures Research Institute, Moscow, Russia.
- Mitchell, J.K. 1964. Shearing resistance of soils as a rate process. *Journal of Soil Mechanics and Foundation Division, ASCE* 90(SM1):29-61.
- Mitchell, J.K. 1976. *Fundamentals of Soil Behavior*. New York, NY: John Wiley & Sons, Inc.
- Mitchell, J.K., R.G. Campanella and A. Singh. 1968. Soil creep as a rate process. *Journal of the Soil Mechanics and Foundations Division, ASCE* 94(SM1):231-253.
- Mitchell, J.K., A. Singh and R.G. Campanella. 1969. Bonding, effective stresses and strength of soils. *Journal of the Soil Mechanics and Foundations Division, ASCE* 95(SM5):1219-1246.
- Murayama, S. and T. Shibata. 1958. On the rheological characteristics of clays. Part I, Bulletin No. 26. Disaster Prevention Research Institute, Kyoto, Japan.
- Murayama, S. and T. Shibata. 1961. Rheological properties of clays. In *Proceedings of the Fifth International Conference on Soil Mechanics and Foundation Engineering*, 1:269-273. Dunod, Paris.
- Murayama, S. and T. Shibata. 1964. Flow and stress relaxation of clays. In *Proceedings of the Rheology and Soil Mechanics Symposium of the International Union of Theoretical and Applied Mechanics*, eds. J. Kravtchenko and P.M. Sirieys, 99-129. New York, NY: Springer-Verlag.

- Noble, C.A. and T. Demirel. 1969. Effect of temperature on the strength behavior of cohesive soil. Highway Research Board Special Report 103, 204-219. National Research Council (U.S.), Highway Research Board, Washington, DC.
- Pan, J-Z. 1986. The general rheological model of paddy-soils in south China. *Journal of Terramechanics* 23(2):59-68.
- Pan, J-Z., G-F. Cai and Y-J. Huang. 1990. The modified rheological model for paddy soils in South China after remoulding. *Journal of Terramechanics* 27(1):1-6.
- Pan, J-Z. and C-Y. Ji. 1987. Prediction of sinkage for wetland vehicles. *Journal of Terramechanics* 24(2):159-168.
- Polivka, M. and C. Best. 1960. Investigation of the problem of creep in concrete by Dorn's method. Internal Report. Department of Civil Engineering, University of California, Berkeley, CA.
- Ram, R.B. and C.P. Gupta. 1972. Relationship between rheological coefficients and soil parameters in compression test. *Transactions of the ASAE* 15:1054-1058.
- Ree, T. and H. Eyring. 1958. The relaxation theory of transport phenomena. In *Rheology*, ed. F.R. Eirich, Volume 2, Chapter 3:83-144. New York, NY: Academic Press.
- Shen, J. and Q. Yu. 1989. Investigation of creep characteristic of wet soils. In *Proceedings of International Conference of Applied Mechanics* 2:1052-1057. Chinese Society of Applied Mechanics, Beijing, China.
- Shen, J. and Q. Yu. 1990. Pressure-sinkage-time equation for wet soil. In *Proceedings of 10th International Conference of the International Society for Terrain-Vehicle Systems* 1:143-148. ISTVS, Hanover, NH.
- Singh, A. and J.K. Mitchell. 1968. General stress-strain-time function for soils. *Journal of the Soil Mechanics and Foundations Division, ASCE* 94:21-46.
- Sudo, S., R. Yasutomi and F. Yamazaki. 1968. The mechanical behaviour of soil and its state of stress. *Journal of the Society for Material Science, Japan* 17:175.
- Vyalov, S.S. 1986. *Rheological Fundamentals of Soil Mechanics*. Amsterdam, The Netherlands: Elsevier Science Publishing Company Inc.
- Wu, T.H., D. Resindez and R.J. Neukirchner, R.J. 1966. Analysis of consolidation by rate process theory. *Journal of the Soil Mechanics and Foundations Division, ASCE* 92(SM6):229-248.